EAI Endorsed Transactions
on Digital Transformation of Industrial Processes Research Article EAI.EU

Modelling an Electro-hydraulic Proportional Valve in a Closed-Loop Control System using Matlab/Simulink

António Ferreira da Silva[1,2], Adriano A. Santos[1,2,*], Filipe Pereira[1,2,3], Carlos Felgueiras[4], António M. Lopes[2,3], Fernando G. de Almeida[2,3], Paulo J. Silva[4] and António Ramos Silva[2,3]

[1]ISEP, Polytechnic of Porto, rua Dr. António Bernardino de Almeida, 4249-015 Porto, Portugal
[2]INEGI - Institute of Science and Innovation in Mechanical and Industrial Engineering, 4200-465 Porto, Portugal
[3]FEUP - Faculty of Engineering University of Porto, 4200-465 Porto, Portugal
[4]CIETI, Polytechnic of Porto, rua Dr. António Bernardino de Almeida, 4249-015 Porto, Portugal

Abstract

In this paper the main components of a hydraulic positioning unit are modelled and simulated using the software Matlab/Simulink. That includes the actuator, the pressure relief valve, connecting pipes and of course the proportional directional control valve. With this model the positioning unit was tested under different conditions to make predictions on how the system is going to react. The simulation of the proportional directional control valve was divided into a static and dynamic part. Based on flow, pressure and leakage curves given by the manufacturer, pseudo-section functions have been created. These functions characterize the relationship between normalized spool position and flow rate. For simulating dynamic behaviour, a non-linear Simulink model was created. The model was fitted to non-linear frequency response analysis (NFR) data points by using a Nelder-Mead simplex optimization algorithm. Several experiments were carried out to test the methodologies as well as the models with the manufacturer's data and experimentally verifying the adjustability of the results and the validation of the approach. The valve model shows high positioning accuracy and robust behaviour in both simulation and experimentation. The amplitude response curves for 10% and 25% showed some oscillation, but with a stable behaviour around the measurement. On the other hand, the amplitude curve for 100% of the coil path showed a very acceptable approximation and even coincided with the manufacturer's curve.

Keywords: Control, Electro-hydraulic actuators, Mathematical model, Non-linear. Position control, Proportional valves, Simulation

Received on 04 March 2025, accepted on 26 March 2025, published on 11 April 2025

doi: 10.4108/dtip.8837

1. Introduction

Hydraulic positioning units are widely used in industrial applications. In general, the positioning unit consists of an actuator, a pressure relief valve (PRV), a proportional directional control valve (PDCV), actuated by a proportional input signal, connecting pipes and pump. On the other hand, the replacement of on-off solenoids with solenoids which can adjust the spool position of a directional valve proportionally to their input voltage was the groundwork for the development of proportional valve technology. So, proportional valves are a good alternative to conventional servo-solenoid valves, since these valves, although highly precise, are very expensive. The robustness and low price of the proportional valve is indeed a good alternative to the servo valves since they are extremely demanding in terms of maintenance and the surrounding industrial environment, i.e., they are a good alternative for application in industrial automation. The use of this type of valve in hydraulic circuits does not exempt it from some internal and external constraints. These are

*Corresponding author. Email: ads@isep.ipp.pt

present in all hydraulic control applications, and which produce uncertainties and non-linearities. These disturbances, however small, influence the robustness and accuracy of the positioning and they cause uncertainties and non-linearities result from friction and internal leakage.

Then, due to the complexity of friction influence at the piston of a hydraulic cylinder [1]-[3], the simulation of the positioning unit must be implemented as a closed-loop circuit [4][5]. In this work, the later-designated components of a hydraulic positioning unit are modelled and simulated using Matlab/Simulink [6][7]. To this end, and for the use of electro-hydraulic actuators, a more in-depth knowledge of the dynamic behaviour of each component is required, in order to characterize these non-linearities and develop an appropriate control law that allows an effective use reaction to be predicted under different conditions [8].

To describe the dynamic behaviour of a technical system, it is important to determine its state variables and energy storages. For this reason, typical energy storages and state variables shall be determined regarding hydraulic systems. Valves are used to control hydraulic systems so, depending on their spool position, they uncover a certain area the oil can pass through [5]. When the valve opens, the resulting flow forces, which act directly on the movement of the gate, affect the dynamic response of the valve which manifests itself on the spool resulting in oscillations. These alter the dynamic characteristics of the valve and the oscillations of the forces generated by the continuously regulated flow. The behaviour of this type of valve is defined by frequency response curves supplied by the manufacturers, which reflect their dynamic behaviour. These amplitude and phase relationship curves are normally presented in the frequency domain but should also be discussed in the time domain [9]-[11].

Therefore, when simulating a hydraulic circuit, oil being the central element of the circuit becomes a very important factor, so the most important properties (viscosity, compressibility, etc.) of the oil must be taken into account when developing the model [5][8][12]. This is why these properties must be properly calculated so that their use in simulation models and can facilitate the creation of static and dynamic relationships that allow simulation models to be created. On the other hand, system modelling must take into account that all constraints cause non-linearities resulting from electrical hysteresis in the proportional valve [13][14], dead-band non-linearities [13]-[16], pressure drops inside the valve and friction in the cylinder [13]-[19] and fluid temperature variations [14][20]-[22].

The organizational structure of this paper is as follows. The principal design of the dynamic behaviour of the system is introduced in Section 2. The mathematic models, simulated and analysed of the PDCV are established in Section 3. The results that are analysed and discussed was made in Section 4. Finally, several conclusions are drawn in Section 5.

2. Analises of the dynamic behaviour of hydraulic systems

A simulation is an important tool in modern technology [23], and it is particularly used in engineering [24]. What makes them so meaningful is the ability to reproduce a real system and make virtual improvements to examine what the impact would be. The real system can be tested under several conditions to make sure that it works appropriately for a particular application. An immense advantage is that systems can be tested before being built without the strict need of a prototype, which saves time and money [25]. Furthermore, it allows the analysis of variant model setups for the behaviour of an individual parameter which clarifies its impact on the result. Simulations also allow observing the behaviour of a system over a very short as well as a very long period. Another important factor is that most real systems cannot be analysed with adequate accuracy due to high complexity. So, five important steps of creating a simulation model shall be introduced in relation to hydraulic systems. These are:

- Drawing a schematic with all input and output signals and coefficients.
- Identifying the energy storages and their state variables.
- Setting up balance equations.
- Complementing missing relations with static equations.
- Drawing a block diagram.

The first step is to draw a diagram of all the important signals entering or leaving the system. In the context of hydraulic systems, the most common signals are pressures and flows, so a representative diagram will provide an insight into the dynamic evolution of the system. In a second step, the system's energy stores must be identified. These indicate where the dynamic system stores the energy contained in the system. A dynamic technical system has one or more energy stores, depending on its complexity. So, the storages can be divided into concentrated and spatially distributed [26].

As a result of this classification, it is necessary to distinguish the forms of energy storage since they will have different representations. Thus, in dynamic systems, concentrated energy storage is presented by state variables that depend on time, while spatially distributed energy storage is described by state variables that depend on time and position. Concentrated energy storage is used more often due to its lower complexity. State variables are closely linked to storage because they describe the amount of energy contained in the storage elements of systems [27]. The state variable is also of high interest because they describe the dynamic behaviour of the system and cannot change abruptly. On the other hand, it should be borne in mind that a state variable is always proportional to the integral of the input parameters and, consequently, are the inputs or integrated blocks in the simulation and, at the

same time, part of the equilibrium equations. For this reason, it is important to determine the equations for balancing forces and torques in translational and rotational masses, as well as the equations for balancing volume flows in capacities. These equations play an important role in hydraulic systems and can be translated, for example, as:

$$F_{acc} = \sum F_{acting} \quad (1)$$

and

$$M_{acc} = \sum M_{acting} \quad (2)$$

Where F_{acc} is the sum of all forces acting on the mass. Forces generated by pressures, springs, friction, or load and they can have positive or negative signs depending on their direction. The same considerations can be applied to the momentum of the balance, M_{acc}, (2) and the volumetric flow rate balance equations can be determined as following:

$$Q_{stor} = \sum Q_{in} - \sum Q_{out} \quad (3)$$

Where Q_{stor} indicates the stored volumetric flow rate, which is the difference between the oil inlet and outlet of a given capacity, and:

$$p = \frac{1}{C_y} \int Q_{stor}\, dt \quad (4)$$

from the fluid state variable computation (4) can be concluded that the pressure change dp/dt is proportional to Q_{stor} when capacity is constant. Where p is pressure and C_y is the capacity of a fluid volume. The last stage consists of the complementation of the missing relationships with static equations, without finalizing the model, which will define the behaviour under stabilized conditions. The system's block diagram, simulation model, can now be drawn based on the equations obtained using Matlab/Simulink.

2.1. Proportional valve operating principle

For mastering the general requirements of today's hydraulic applications valves are indispensable. Valves satisfy different tasks in hydraulics, and they are categorized in four different classes. These are: pressure valves, flow-control valves, check valves and directional valves [28]. Pressure valves limit or restrict a certain pressure level respectively a pressure difference. Flow-control valves spread or restrict the flow rate as required fort the application. Check valves have the task to block the flow rate in one or even both directions and repeal it under some specific circumstances. Directional valves are used to control the direction of the flow rate. Each of these four classes is also divided in many more sub types.

The last group of valves is one of many electrically operated hydraulic valves and are directional valves with improved control electronics. The control electronics ensure that the force developed by the coil can be adjusted continuously and with remarkably high precision by means of an input voltage or current. This feature is necessary when they are used in high-precision hydraulic control circuits. These valves can be divided into servo valves and proportional valves [29].

In a servo valve, a torque motor is used to control the position of the servo valve coil via several amplification stages. Most of the time, it has two or three motors in order to use a very low input signal and be able to control huge output signals [30]. This type of valve is used in high-precision applications and places high demands on the working environment. In order to achieve these accuracies, a very precise level of valve functionality is required, and the manufacturing must also be precise. This makes this type of valve expensive. In contrary to that are proportional valves which are effectively a further development of directional valves with simple switching solenoids. Proportional valves are widely spread in automation engineering because of their robustness and cheapness compared the servo valves [31].

Due to the high precision, it is possible to achieve adjustment of all four control edges around the working point at the same time. The others are closed or opened in such a way that the restriction effect has no impact compared to the relevant control edge. This allows for higher manufacturing tolerances when producing the control edges. Proportional valve technology is used in direction, pressure, and flow valves. When using proportional directional control valves, it is necessary to have stroke-controlled magnets that can adjust the position of the coil continuously without any problems. This makes it possible to have the function of an additional flow control valve, which is important for achieving a correct actuator position in position control applications. Figure 1 illustrates the proportional valve used in this hydraulic system. The parts marked "a" and "b" are the proportional solenoids that are used to move the control spool [32].

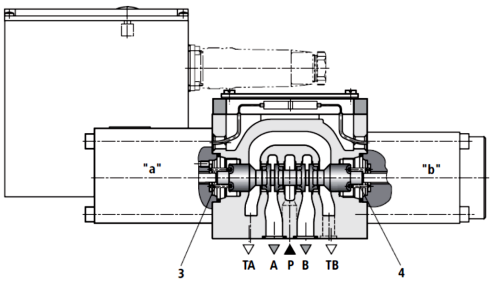

Figure 1. Proportional Valve Bosch Rexroth 4WRSE

When both solenoids are conducting, their forces are equalized and the springs "3" and "4" centre the spool, the same happens when the solenoids are not conducting. For positive displacement of x, the proportional solenoid "b" must be active whereas "a" must be active for the other direction. Inductive displacement measurement detects either positive or negative spool position and compensates

widely the position error caused by friction and spring fatigue.

The applied technology of displacement measurement in proportional valves is called "Linear Variable Displacement Transformer" or LVDT. The LVDT consists of a coil assembly and a core. The coil assembly is typically mounted to a stationary form, while the core is secured to the object whose position is being measured. The coil assembly consists of three coils of wire wound on the hollow form. A core of permeable material can slide freely through the centre of the form. The inner coil is the primary, which is excited by an AC source. Magnetic flux produced by the primary is coupled to the two secondary coils, inducing an AC voltage in each coil. The main advantage of the LVDT transducer over other types of displacement transducer is the high degree of robustness. Because there is no physical contact across the sensing element, there is no wear in the sensing element. Because the device relies on the coupling of magnetic flux, an LVDT can have infinite resolution. Therefore, the smallest fraction of movement can be detected by suitable signal conditioning hardware, and the resolution of the transducer is solely determined by the resolution of the data acquisition system [33] In Figure 2 the measurement system is illustrated [34]. In the left part of the figure the entire inner construction is shown. In right part of the figure, the LVDT is emphasized with the red circle.

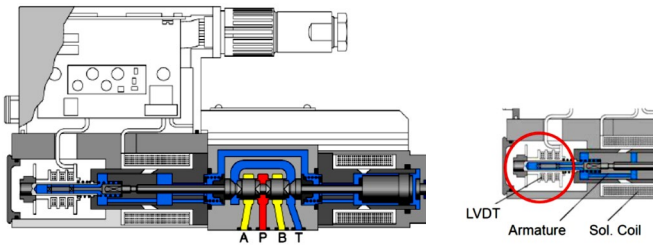

Figure 2. LVDT of the Proportional Valve Bosch Rexroth 4WRSE

3. Modelling the Electro-Hydraulic Proportional System (EHPS)

The electro-hydraulic proportional system modelled (see Figure 3) consists of a double acting cylinder (4), a pressure relief valve (2), a proportional 4/3 directional valve (3), a fixed displacement pump (1) and pipe connections. Therefore, a sensor measures the cylinder position and transfers that information to a controller. The controller compares the actual position of the cylinder with the desired position the cylinder is supposed to have. If they are not equal the controller gives an electric signal in the range from -10 V to +10 V to the proportional valve. The voltage input is the command signal which dictates the opening stroke of the proportional valve. In this case -10V refers to -100% open according to maximum spool stroke whereas +10V results in a +100% open valve.

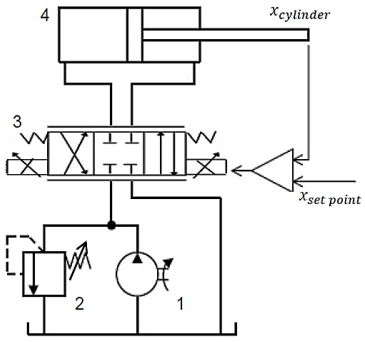

Figure 3. Electro-Hydraulic Proportional System

When the desired position is reached and the system is stabilized, the valve is adjusted in middle position and blocks the cylinder. That would cause high pressure and damage the system. To prevent the system from damage caused by an enormous pressure level, the pressure relief valve is used. It opens when pressure is getting beyond a certain level and allows oil to drain to the tank. An overview of the system is illustrated in Figure 3.

3.1 Modelling Hydraulic Cylinder

The problems associated with electro-hydraulic systems are classified as position control, speed control and force control. The most common applications for this type of proportional electro-hydraulic drive are associated with positioning, speed, force, or torque, whether for linear or angular movements. In this section, the theoretical considerations regarding the dynamic behaviour of the cylinder are explained. Based on these considerations, a control model was created for a differential cylinder with the dimension 200-100-500, where the piston diameter in mm is 200, the rod diameter is 100 and the stroke is 500, respectively. So, in this research, determining the dynamic behaviour of the system is the first step to building the model. Figure 4 illustrates the model of the differential cylinder with inflow and outflow port to the two-cylinder chambers. For the setup shown it is assumed that the piston extracts.

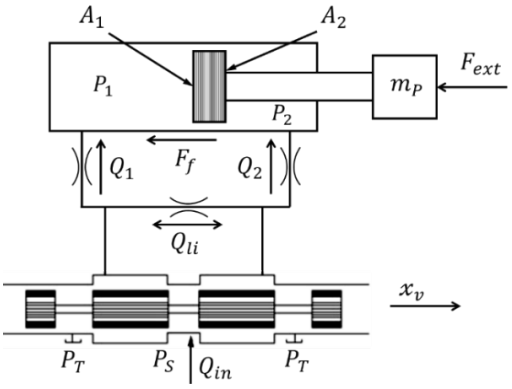

Figure 4. Differential cylinder model

The proportional directional valve is supplied by pressure (P_S). The hydraulic cylinder is supplied by a flow rate (Q_1) and a flow rate (Q_2) which are a function of the valve spool position (x_v), given by the valve's LVDT, and the pressures (P_1) and (P_2). In addition, the pressure in both chambers of the double-acting cylinder can differ from the pressure in the pipes connecting to the valve. However, the pressure drop between the chamber and the pipe is insignificant compared to the high nominal pressures in the chamber. Furthermore, the volume of the pipe can be added to the volume of the cylinder (V_1) and (V_2) to avoid a rigid system. If the piston is accelerated, there is no static behaviour and the pressure levels in the chambers are different from in the connected pipes. When the system reaches a static state, the speed of the piston is constant and inflow and outflow rate as well.

The cylinder's energy storage is the chambers and the piston mass. The chambers store fluidic energy where pressure can be obtained from. Whereas the piston mass stores kinetic energy where acceleration, velocity and displacement can be obtained from. For the derivatives of pressure p_1 and p_2 (pressure dynamics equations) can be written by:

$$\dot{p_1} = \frac{1}{C_1}(Q_1 - Q_{V1} - Q_{li}) \tag{5}$$

$$\dot{p_2} = \frac{1}{C_2}(Q_{V2} + Q_{li} - Q_2) \tag{6}$$

where C_1 and C_2 are, respectively, the capacity of the chamber 1 and 2. Q_1 and Q_2 are the flow rates which stream in and out of each chamber. Q_{V1} and Q_{V2} are the flow rates in each chamber and Q_{li} are the leakage flow rate. The incoming flow rate Q_1 which depends on the restriction and the pressure difference between chamber and pipe. The inlet flow rate must have the same amount of the outlet flow rate. When the difference is not balanced, the pressure increases or decreases. Them, when there is a certain flow rate Q_1 streaming into the chamber, the same amount must flow out. However, when the pressure level remains the same, capacity must increase. On the other hand, with the assumption of an almost constant bulk modulus, capacity can only increase when volume increases. Them, flow rate Q_{V1} must be considered in that equation. It does not drop out but increases the volume. Likewise, the leakage flow rate Q_{li} must be considered as well. It results from the pressure difference between the chambers and cannot be avoided because of dimensional tolerances in the manufacturing process. A laminar flow profile is assumed in the leakage gap. From these considerations follows:

$$Q_1 = sign(p_{in} - p_1)\, k_{dr1}\, A_{dr1}\sqrt{|p_{in} - p_1|} \tag{7}$$

$$Q_{v1} = \dot{x}\, A_1 \tag{8}$$

$$Q_{li} = G_g\, \Delta p_{12} = \frac{\pi \cdot d_m \cdot h^3}{12 \cdot \eta \cdot l_k}\, \Delta p_{12} \tag{9}$$

where p_{in} is the pressure at chamber inlet, k_{dr1} is the throttling coefficients for cylinder inlet flow rate, d_m is the mean diameter of the cylinder, η is the dynamic viscosity, l_k is the length of the piston and Δp_{12} is the pressure difference between chambers 1 and 2. The hydraulic capacity of the chamber C_1 and C_2 are given by:

$$C_1 = \frac{K_b(p_1)}{V_1} = \frac{K_b(p_1)}{V_{1,0} + x \cdot A_1} \tag{10}$$

$$C_2 = \frac{K_b(p_2)}{V_2} = \frac{K_b(p_2)}{V_{2,0} - x \cdot A_2} \tag{11}$$

where $V_{1,0}$ and $V_{2,0}$ are the volumes for a retracted cylinder position. Thereby $V_{1,0}$ is the dead volume of the cap end chamber and $V_{2,0}$ characterizes the dead volume of the rod end chamber plus the volume $x \cdot A_2$. The dead volumes are assumed as 1% of the total piston volume. K_b is the bulk modulus for fluids, is equivalent to the modulus of elasticity for solid structures, and it is assumed to:

$$K_b\big(p(t)\big) = K_{b,max}\big(1 - e^{-n \cdot p(t)}\big) \tag{12}$$

where $K_{b,max}$ is set to 1.2E^{-9} Pa and $n = 4.6052\text{E}^{-6}$, considering a kinematic viscosity of $\nu = 46\ mm^2/s$. As a consequence, the force balance equation must also contain all relevant forces. So, the equation can be written as:

$$\begin{aligned} m\ddot{x} &= F_1 - F_2 - F_f - F_L \\ m\ddot{x} &= (p_1\, A_1) - (p_2\, A_2) - F_f - F_L \end{aligned} \tag{13}$$

where F_1 and F_2 are the force in chamber 1 and 2. The friction force is F_f and F_L the load force. Friction results when the piston displaces in the cylinder body. This happens due to the contact between piston and the cylinder wall. Thereby the influence of static, dynamic, and viscous frictions must be considered in the same way. Viscous friction is caused by the leakage gap between cylinder wall and piston. According to [35] the influence of friction must be considered especially in feed-back systems. For instance, when the static friction is very high, the system is not able to act on small pressure differences. Firstly, static friction must be overcome. For high piston velocities a huge extract of energy or a high damping can be a result. The exact advance projection is not possible. For this reason, the friction force is measured on the real system. Different pressure differences at diverse speeds must be collected for only one direction of movement. With that set of data, the coefficients of a regression polynomial can be determined in a way that the polynomial fits the real measured behaviour. Thereby, the objective is to determine the dimension of these forces. During the simulation, certain values can be varied to obtain better results. When high accuracy is needed, a polynomial for each direction of movement must be created. According [35], the friction force on a piston can be characterized as following:

$$F_f(\dot{x}) = sign(\dot{x})\left[F_{df} + F_{sf}\, e^{-\frac{|\dot{x}|}{T_v}}\right] + k\, \dot{x} \tag{14}$$

where F_{df} is the dynamic and F_{sf} the static friction. T_v is the decay constant and k the coefficient of viscous friction. The static friction term decreases exponentially with increasing speed, while the viscous friction remains constant and proportional to speed. On the other hand, due to the assumption of a laminar flow profile in the leakage gap, the k factor can be determined as follows:

$$k = A\,32\,\frac{\eta \cdot l_k}{d_m^2} \tag{15}$$

where η is the dynamic viscosity, d_m the mean diameter and l_k is the length of the piston. Dynamic friction, F_{df}, and static friction, F_{sf}, is given by:

$$F_{sf} = \mu_{sf}\,F_N \tag{16}$$

$$F_{df} = \mu_{df}\,F_N \tag{17}$$

Since, it is not possible to measure the friction force of the real cylinder shall be used. The static and dynamic friction forces shall be determined based on normal force. The normal force of the piston is 330 N due to its weight, and the friction coefficients are $\mu_{sf} = 0.12$ and $\mu_{df} = 0.05$.

Based on the theoretical equations presented above, the Simulink model of the differential cylinder shown in Figure 5 was created. It was assumed that the proportional valve has already reached a fixed position and that the pressure levels in the inlet and outlet pipes are constant.

The equation (7) to (9) characterize the input in the left chamber. Pressure builds up and the piston extends. To model the march of pressure (5) and (6) is used, Figure 6. Pressure $p1$ and $p2$ are each modelled in a subsystem.

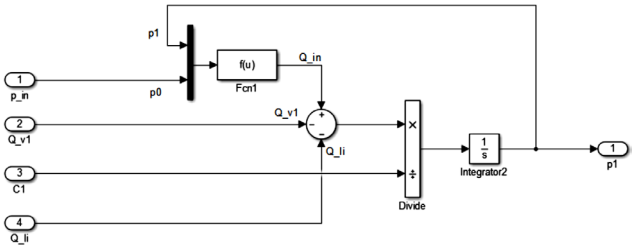

Figure 6. Pressure dynamics of the left side Simulink model (chamber 1)

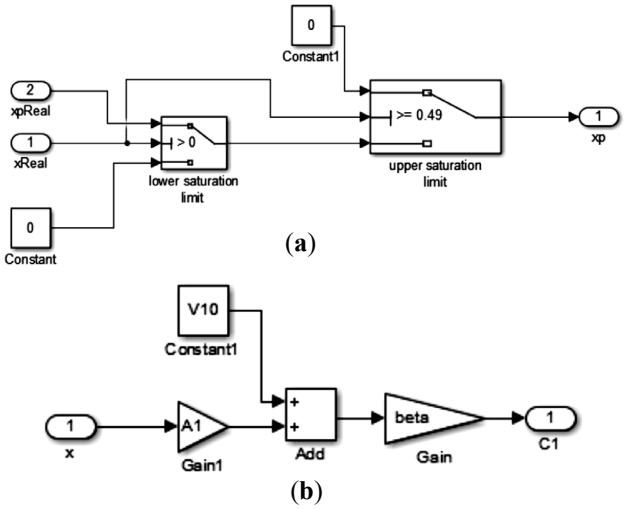

Figure 7. Subsystems of chamber Simulink model: (a) velocity saturation, (b) capacity C_1.

Capacity and velocity are modelled in a subsystem as well. It changes with a different spool position. The maximum spool position was determined to 49 mm. The input for the

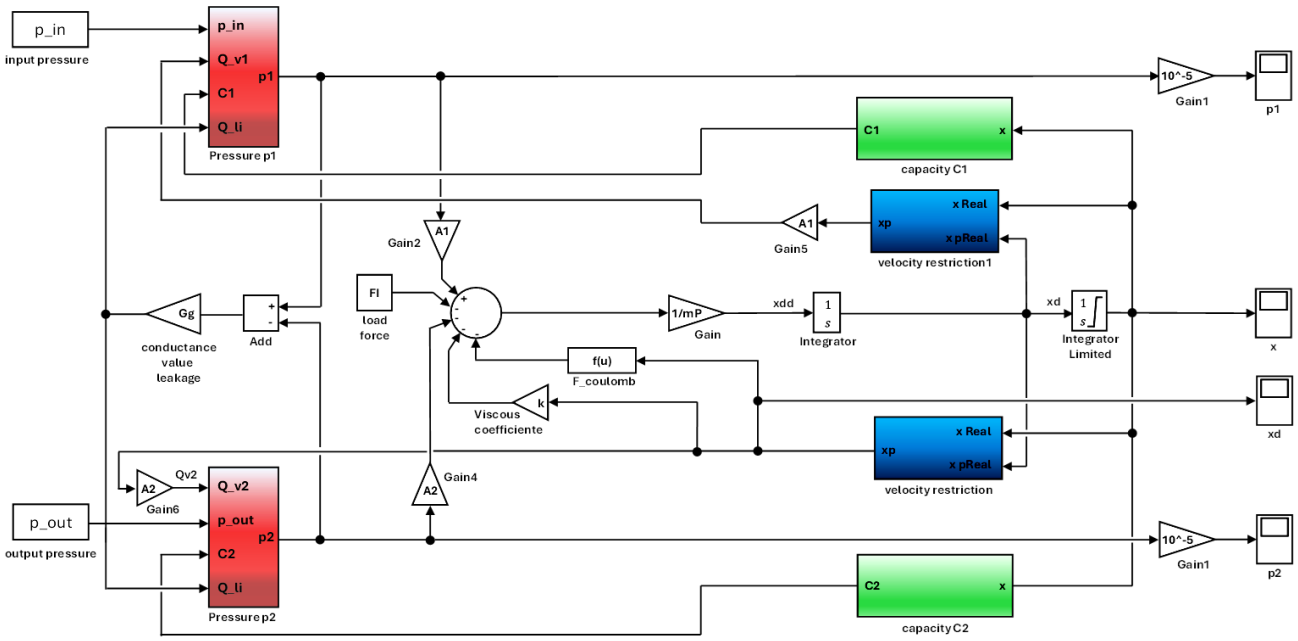

Figure 5. Double acting cylinder Simulink model

capacity subsystems is the limited velocity. Two switch-case blocks are used to set the velocity to zero when the spool position is out of range of motion. All subsystems are illustrated in Figure 7.

Similar considerations can be made for the right piston chamber. Pressure is modelled as a sub-system (Figure 8) and the capacity model for chamber 2 is presented in Figure 9. The velocity saturation of the chamber 2 is de same presented in Figure 7(a).

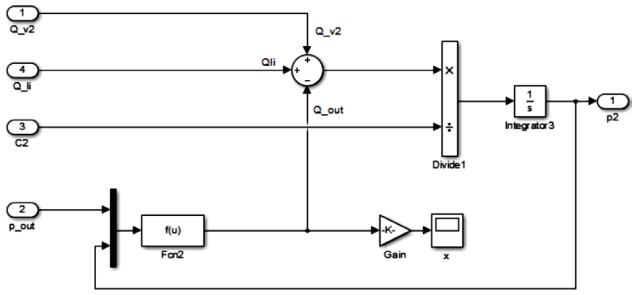

Figure 8. Pressure dynamics of the right-side Simulink model C_2.

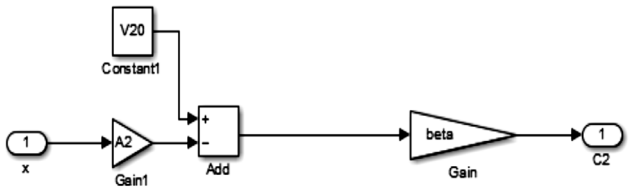

Figure 9. Subsystems of chamber Simulink model, capacity C_2.

3.2 Proportional Directional Valve Model

To create the dynamic simulation of the proportional valve, type 4WRSE-10V with four-way spool, its behaviour was divided into two parts: the dynamic part and the static part. The dynamic part provides information on how quickly the valve can react to a step response, i.e., how quickly the coil can react to a given input signal. The static behaviour provides information on the flow and pressure characteristics at a given coil position. Based on this, Yuan et al. [11] developed a study of the behaviour of the electromagnetic subsystem of a proportional valve, establishing models that portray the non-linear dynamic performance considering structural parameters such as materials, fluids, and interaction strategies with the other subsystems. However, [36] using a hydraulic servo system, developed a non-linear simulation model in Matlab/Simulink, in a closed loop, using fractional order controllers, genetic algorithm (GA), which takes into account the friction between the cylinder and the piston, the compressibility of the fluid, the dynamics of the valves and the influence of uncertainties such as pressure, Coulomb friction and viscous friction. On the other hand, [36] presents a model of a hydraulic servo system using particle swarm optimization techniques. The model also includes non-linear effects to study the dynamics of the system and the effects of forces and oil compressibility on the performance of its dynamic and non-linear behaviour. The results obtained were promising and satisfactory. Them, to modelling an Eaton Vickers KBSDG4V-3 proportional valve [37] adopted a two-part modelling approach. First studying the static behaviour (flow gain, pressure gain and leakage flow) followed by the dynamic behaviour (frequency response) of the valve. The approach, based on the manufacturer's characteristics, provided good results that were fairly accurate and close to the real frequency characteristics. On the other hand, the dynamic behaviour of the proportional valve used, Bosch Rexroth 4WRSE-10, has slightly different dynamic characteristics. It does not show any amplitude gain behaviour at certain frequencies, unlike the Vickers valve. However, this approach was applied to the value not only to test its applicability, but also to obtain the same good results.

Dynamic model

Modelling dynamic behaviour by using basic theoretical foundation would lead to imprecise results due to the complexity of the valve. For this reason, a different approach shall be applied. The non-linear frequency response data given by the manufacturer shall be used because they represent the proper dynamic behaviour of the valve. That implies that this approach provides specific results only relating to that valve type. It doesn't provide general results for different types of valves.

The curves are extracted from the datasheet, a typic Bode diagram for the Bosch Rexroth, is shown in Figure 10 [32]. It measures the amplitude response as well as the phase angle for three different normalized input signals of ±10%, ±25% and ±100% of maximum spool stroke. Since the data is valid for positive and negative spool position, symmetrical valve behaviour can be suggested. There is measured data over the whole displacement range of the spool. That provides a good understanding of the real valve behaviour which makes these curves appropriate to build a simulation on.

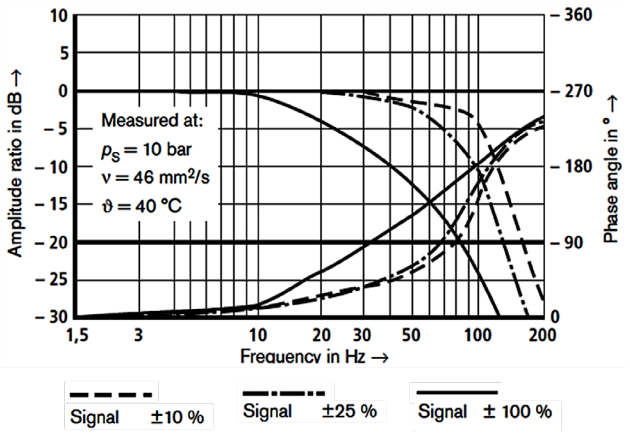

Figure 10. Amplitude and phase response curves

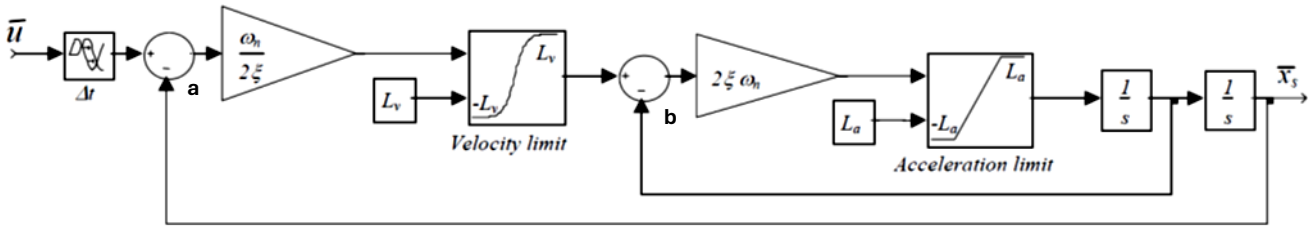

Figure 11. Non-linear dynamic model of spool position of the valve [37]

Due to the non-linearity of the system, the Simulink model that translates the curves presented above showed a different output behaviour to that plotted in the characteristic curves when fed with different input amplitudes. These deviations are important because they reflect an expected dynamic behaviour, validating them when tested with different inputs.

Therefore, according to [37], a second-order linear system was used which had to be optimized to obtain the desired behaviour. Otherwise, the non-linearity could not have been realized. As already mentioned, the valve's characteristics are the same for positive and negative coil displacements. It was also assumed that the real valve has limitations for velocity and acceleration (positive and negative directions), since they cannot be infinitely large. Finally, it is assumed that the curves are not measured absolutely but normalized to the maximum travel of the coil. There is therefore no need for a stationary gain factor because it is equal to one. The non-linear equation for the system, transposed for the highest derivative of x, can be determined as follows:

$$\ddot{x} = \frac{u(t)}{m} = -\frac{d}{x}\ddot{x} - \frac{c}{m}x$$
$$\ddot{x} = K\,\omega_n^2\,u(t) - 2\zeta\omega_n\dot{x} - \omega_n^2 x \quad (18)$$

where u is the input variable in order of time (t), m is the mass, d the damping constant and c the spring constant, K is the gain factor and ω the natural frequency. The ζ is the damping factor and is given by:

$$\zeta = \frac{d}{2\sqrt{m\,c}} \quad (19)$$

According to (18) and [37], the model created in Simulink can be represented as shown in Figure 11. In this model, the frequency response is modelled with a second order system with velocity and acceleration saturation. However, there is no stationary gain factor on the left, which confirms the previous explanations. You can also see that the delay block is used to obtain the phase lag. The rest of the model is used to obtain the amplitude response behaviour.

The parameters of the model shown in the previous figure were estimated using an optimization algorithm with least squares cost function, where L_v is the limit velocity and L_a the limit acceleration. As a result, it was possible to create equilibrium equations at the sum points "a" and "b", in Figure 11, obtaining the following:

$$a = \bar{u} - \bar{x} \quad (20)$$

and

$$b = a\,\frac{\omega_n}{2\zeta} - \dot{x} \quad (21)$$

Additionally, the acceleration can be written as:

$$\ddot{x} = b\,.\,2\,\zeta\omega_n \quad (22)$$

By replacing "a" and "b" in (22) and expanding them, the acceleration can be written as follows:

$$\ddot{x} = u(t)\omega_n^2 - 2\,\zeta\omega_n\dot{x} - \omega_n^2\,x \quad (23)$$

By comparing the coefficients of (18) and (23), it can be determined that both equations are equal except the gain factor K.

The model in Simulink is created with general variables as it is shown in Figure 11. This model shall be fit to the measurement curves from the manufacturer. Therefore, the data points must be available in Matlab.

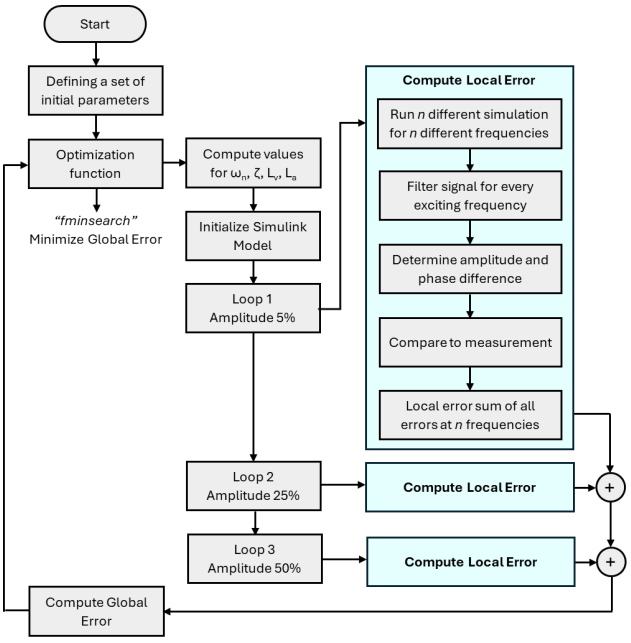

Figure 12. Optimization of dynamic model

If the model is simulated with certain initial values, there is an error resulting between the measurement points and the simulation values at any frequency of the three amplitude responses. This is since the chosen initial values most likely don't represent the dynamic behaviour. But there must be values for the Simulink model which minimizes the error between measurement and simulation. Additionally, these values represent the best dynamic behaviour the model can achieve. The fact that the error deviation is strongly connected to the model parameters leads to the conclusion that the error sum at each measuring point must be minimal to obtain good parameters for the model. This leads to an optimization problem. To solve optimization problems, Matlab offers various functions which optimize target values with different kinds of implemented algorithms.

The optimization function used in this work is "*fminsearch*" which optimizes non-linear problems without using derivatives. It is based on the Nelder-Mead simplex algorithm [38]. To execute the simulation, initial values are necessary. That influences the simulation duration considerably when far from the final values. Hereafter shall be described how the implemented optimization algorithm works.

The calculation of amplitude and phase must be done separately. Thereby the phase shift is acquired by using a pure time delay. The rest of the model is used to compute the amplitude response. The following flow chart in Figure 12, only refers to the amplitude response computation.

Firstly, the initial values for ω_n, ζ, L_v und L_a must be determined. These initial values are passed to the optimization function. The optimization function manipulates the initial values due to the result of the target function. In this case, the target function is the sum of all squared error deviations. For the first iteration step the system must be simulated completely to achieve a target function value for the initial values. Based on their inner algorithm *fminsearch* decides which initial value must be manipulated and how much. Next the model can be simulated again and the impact on the target function can be examined.

When the optimization function changed the initial values, they were passed to the Simulink model. As illustrated in Figure 12, the simulation is divided into three parts. This is due to the three different input amplitude curves. The result of each of these blocks is the sum of all local squared errors from measurement to simulation point

Table 1. Measured amplitude and phase data points for 4WRSE-10

Frequency [Hz]	Φ at 10% [dB]	Φ at 25% [dB]	Φ at 100% [dB]	A at 10% [dB]	A at 25% [dB]	A at 100% [dB]
1.5	0.0	0.0	0.0	0.0	0.0	0.0
2.0	-4.0	-4.0	-4.5	0.0	0.0	0.0
3.0	-6.0	-6.0	-6.3	0.0	0.0	0.0
4.0	-7.0	-7.0	-8.1	0.0	0.0	0.0
5.0	-7.5	-7.5	-9.0	0.0	0.0	0.0
6.0	-7.6	-7.6	-9.9	0.0	0.0	0.0
7.0	-7.9	-7.9	-9.9	0.0	0.0	0.0
8.0	-8.3	-8.3	-10.8	0.0	0.0	0.0
9.0	-8.6	-8.6	-11.7	0.0	0.0	-0.5
10.0	-9.0	-9.0	-12.0	0.0	0.0	-0.9
15.0	-14.5	-14.5	-31.5	0.0	0.0	-2.0
20.0	-20.7	-23.4	-54.0	0.0	0.0	-4.0
25.0	-26.1	-27.9	-63.0	0.0	-0.5	-5.5
30.0	-36.0	-36.0	-82.0	0.0	-1.0	-7.5
40.0	-44.1	-45.9	-103.5	-1.0	-1.5	-10.0
50.0	-54.0	-62.1	-124.2	-1.3	-2.0	-12.5
60.0	-67.5	-76.5	139.5	-1.7	-3.5	-14.5
70.0	-76.5	-94.5	-148.5	-2.0	-5.5	-16.5
80.0	-90.0	-119.7	-162.0	-2.5	-6.8	-19.5
90.0	-112.5	-148.5	-175.5	-3.0	-8-5	-22.0
100.0	-139.5	-157.5	-184.5	-4.5	-10.5	-24.0
110.0	-171.0	-184.5	-193.5	-7.0	-14.5	-27.5
120.0	-184.5	-193.5	-202.5	-9.5	-15.5	-28.5
130.0	-198.0	-207.0	-211.5	-13.0	-20.0	-31.0
140.0	-207.0	-216.0	-216.0	-15.0	-22.8	-
150.0	-211.5	-220.5	-220.5	-17.0	-25.0	-
160.0	-216.0	-225.0	-225.0	-20.0	-28	-
170.0	-220.5	-229.5	-229.5	-22.5	-30.0	-
180.0	-225.0	-231.3	-234.0	-25.5	-	-
190.0	-225.5	-233.0	-238.5	-26.7	-	-
200.0	-226.5	-234.0	-243.0	-28.0	-	-

at a certain frequency. Global error is computed as following:

$$F_{global} = 4\,F_{local,10\%} + F_{local,25\%} + F_{local,100\%} \quad (24)$$

The local error deviation $F_{local,10\%}$ is weighted with a factor of 4. This is because the valve works most of the time around the middle position to adjust the flow very precisely when controlling the position of an actuator. It is therefore necessary to make a greater effort to get a good approximation of this curve.

The local error was first calculated based on the amplitude response measurement data at different frequencies, taken from the datasheet. The measurement amplitude data (A) and the phase data points (Φ) used is shown in Table 1.

Therefore, feeding the model with a sinusoidal signal led to the appearance of non-linearities resulting from saturation blocks. These blocks, although fundamental for adjusting the model to non-linear curves rainfall, directly influence the optimization of the system. However, this influence is not confined solely to optimization but extends to the output signals since other frequencies appear in their spectrum. These harmonics cause unstable amplitude behaviour due to their overlap with the excitation frequency. This makes it impossible to obtain stable oscillation behaviour, so it is necessary to calculate the amplitude response. For this reason, the simulated output signal must be filtered for a given excitation frequency. After filtering, the output signal is assumed to have a constant amplitude. Consecutively, the ratio between the output amplitude and the input amplitude (A_{output} and A_{input}) at each excitation frequency can them be calculated using (25).

$$A^{[dB]} = 20\,log_{10}\left(\frac{A_{output}}{A_{input}}\right) \quad (25)$$

This result can then be compared with the measurement and the local error can be determined.

$$F_{local} = \sum_{i=1}^{n}\left(A_{measur}\,f(i) - A_{local}\,f(i)\right)^2 \quad (26)$$

Then, the solution vector will be obtained when the minimum of the objective function is determined by the optimization function. In this case, the optimization of the delay time promotes the change of phase depending on the values of the solution vector ω_n, ζ, L_v and L_a.

Signal filtering

The output signal is filtered based on the excitation frequency, the vector of initial values and the normalized input amplitude, returning the simulation time, the input signal, and the filtered output signal. Thus, the higher the excitation frequency, the higher the sampling frequency and, for frequencies that are too low, aliasing can occur, since only two base sampling frequencies are used in the transformation to the frequency domain using the Fast Fourier Transform (FFT). The FFT algorithm, calculated with a fixed step size, transforms the output signal, determined by the Simulink model, resulting in a reflected spectrum at the Nyquist frequency. Furthermore, the fact that the Nyquist frequency is half the sampling frequency means that it is sufficient to trace only half the spectrum up to the Nyquist frequency. The spectrum is normalized by its maximum value, which in this case represents the maximum value of the excitation frequency. Figure 13 shows the output signal of the Simulink model for the simulation values of $\omega_n = 1000\ rad/s$, $\zeta = 0.8$, $L_v = 50$ and $L_a = 50000$. The excitation frequency is set to 180 Hz, so the signal is sampled at 212 Hz, which leads to a Nyquist frequency of 2048 Hz.

However, due essentially to the non-filtering of the output, the results obtained showed an overlapping of the signal and a signal combined with other frequencies due to the non-linear saturation blocks making the amplitude quite unstable. The signal was filtered using analogue band-pass filtering techniques which, due to the inadequacy of their characteristics for this problem, quickly became unstable when they became too narrow. A digital finite impulse response (FIR) filter was therefore used, which operates with cut-off frequencies normalized to the Nyquist frequency. It will be determined by:

$$\omega_{2,1} = \frac{2 \cdot f}{f_s} \pm 0.0001 \quad (27)$$

In addition, the order of the filter is determined with 1 in the numerator and 5000 in the denominator in order to exclude interference frequencies. Figure 13 shows the output signal of the Simulink model for the simulation values of $\omega_n = 1000\ rad/s$, $\zeta = 0.8$, $L_v = 50$ and $L_a = 50000$. The excitation frequency is set to 180 Hz, so the signal is sampled at 212 Hz, which leads to a Nyquist frequency of 2048 Hz.

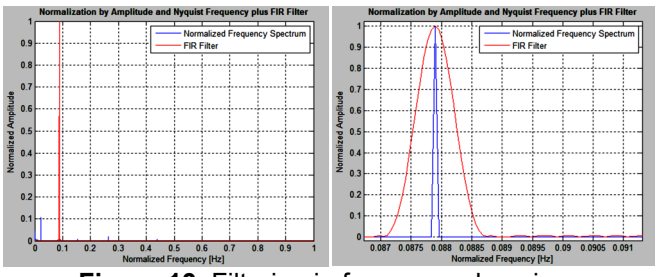

Figure 13. Filtering in frequency domain

According to the graphs in the figures above, it can be seen that the FIR filter gives good results. Even interference frequencies that are close to the excitation frequency can be filtered out very well due to the high order and narrow cut-off frequencies. The filtered output signal must be inversely transformed to the time domain. As you can see in Figure 14, the harmonics have been completely excluded

from the previous signal. The filtered signal can therefore be used to determine the amplitude and phase shift.

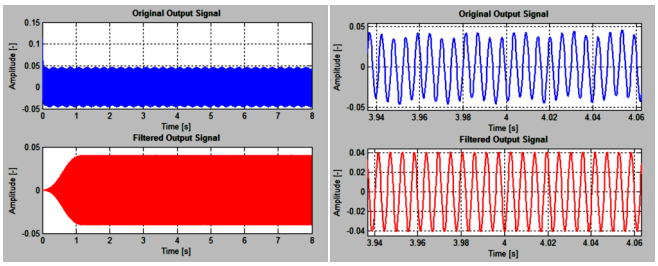

Figure 14. Filtering in signal in time domain

Compute amplitude and phase shift

This section aims to show how the function calculates the steady-state amplitude of the output signal of a dynamic system and determines the phase change in relation to the input signal. So, the algorithm used compares several consecutive amplitudes and determines whether the difference between them is acceptably small and whether steady-state oscillation is achieved. However, this matching of amplitudes is not the only criterion used. In addition, the area under two consecutive half-waves with the same signal must be identical, even if they do not reach a stable oscillation (Figure 15). For this reason, the integration between two points of intersection must also be considered.

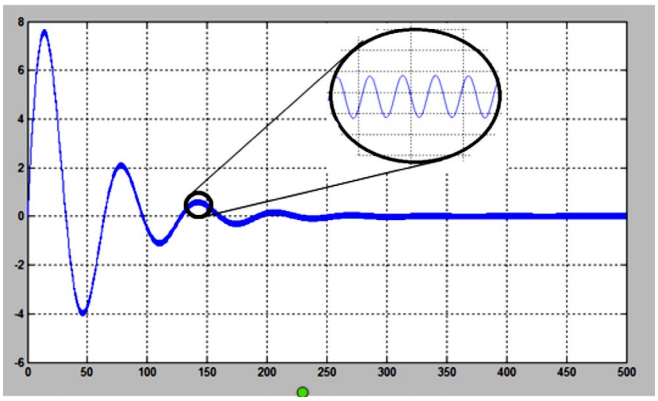

Figure 15. Checking for Steady-State Amplitude behaviour

So, in order to compare the amplitudes and calculate the integrals, the algorithm has to check the largest current amplitude or that of the next step. For each of the iteration steps, the function detects the largest amplitude, setting it to 100 per cent and calculating the maximum possible deviation, which is 0.05 per cent less than the largest amplitude. If the difference found is less than 0.05 per cent of the absolute value, steady-state oscillation is reached and the steady-state amplitude at the time step is found. Due to the fact that the system always oscillates with at least the same phase, but never with a main phase, this calculation method can also be applied to any system, even with a phase deviation of almost 360°. Figure 16 shows the behaviour of the function when applied to systems with a phase deviation of less than 360°.

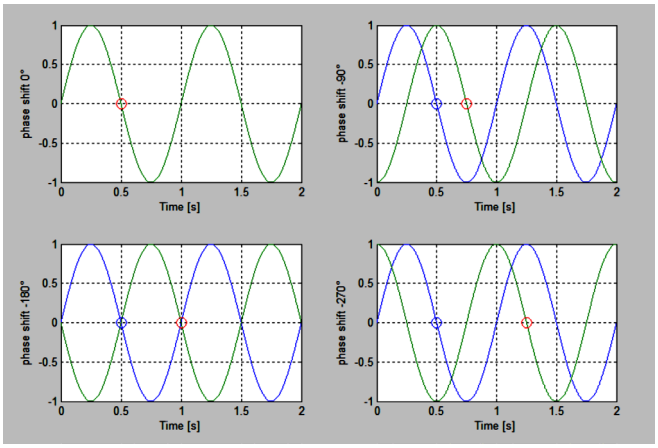

Figure 16. Influence of Phase Shift

Optimization

To optimize the second-order linear transfer model, the parameters for the gain factor K, the damping factor ζ and the appropriate angular frequency ω_0 must first be defined. For a general second-order linear system, we can consider the following:

$$A(\omega) = |G(j\omega)| = \frac{K \cdot {\omega_0}^2}{\sqrt{({\omega_0}^2 - \omega^2)^2 + (2\zeta\ \omega_0\ \omega)^2}} \qquad (28)$$

with, K=5, ζ=0.8 and ω_0=50.

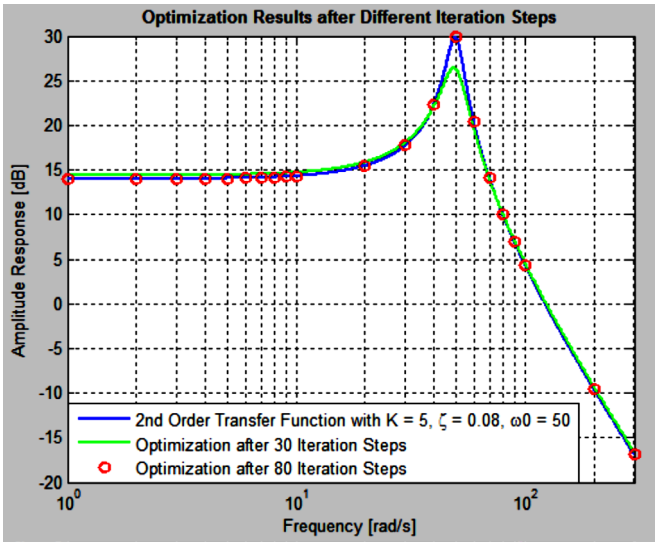

Figure 17. Optimization result linear system

The system can thus be simulated over a wide range of frequencies. The general second-order system was

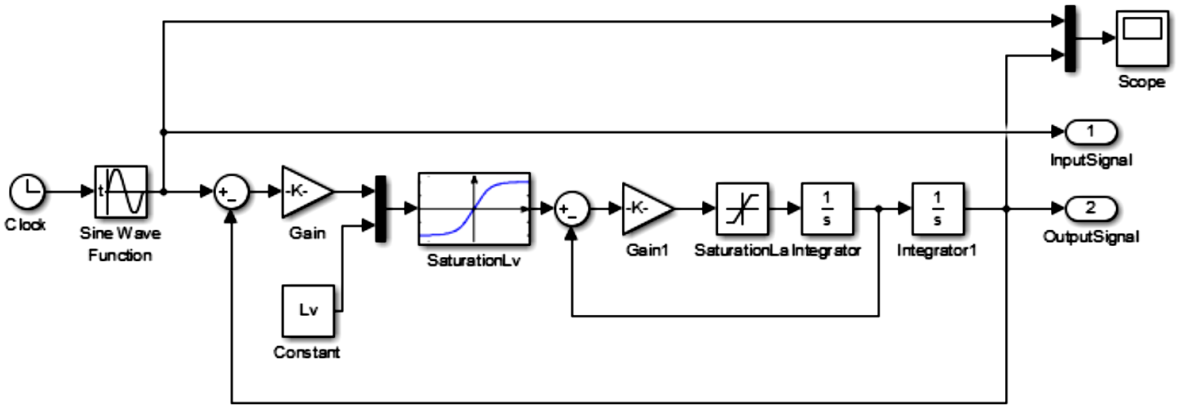

Figure 18. Complete Simulink Model of the Proportional Valve

optimized for these data points. The results show optimization obtained for a maximum of 30 and 80 iterations. Filtering was not necessarily due to the linearity of the transfer function, as show in Figure 17.

Figure shows that after 30 iteration steps, a good approximation can already be seen. However, the area around the natural angular frequency is not well approximated. Slight deviations are recognizable. The simulation results for an optimization after 80 iteration steps are illustrated in red. It can be seen that there is a very good and noticeable approximation. This confirms that the implemented functions work correctly.

The model shown in Figure 11 does not have two general limit blocks with a sudden saturation, which limits the object function. To improve the behaviour of the model, two saturation blocks were used to limit the speed, smooth saturation, combined with a sudden saturation block, to limit the acceleration, and thus minimize the object function as much as possible. In this case, smooth saturation must be obtained using an exponential function with a negative exponent similar to the behaviour of the step response of a PT1 element [39]. The general equation for determining the behaviour of the step response is as follows:

$$a(t) = K\left(1 - e^{\frac{t}{T_V}}\right) \tag{29}$$

where K value represents the final gain value that the function is reaching. T_V is the time constant that indicates the time the function needs to reach 63% of its final value, the decay constant in m/s. The complete Simulink block diagram simulation model is shown in Figure 18.

Figure 19 shows the simulation results of the Simulink model and the comparison with the measurement curves of the Bosch 4WRSE-10 valve. It can therefore be concluded that the implementation of the non-linear Simulink model, as well as its belonging function, are close to the curves considering the optimization parameters ω_0 = 336.7663 rad/s, ζ = 0.4542; L_v = 77.14 s^{-1} and L_a = 128.700 s^{-2}.

Depending on these parameters, we can see that there is an oscillation in the simulation values around the measurement. The curves for the 10% and 25% amplitude ratios show a greater oscillation, but with a stable behavior around the measurement. The amplitude curve for 100% of the coil path are a very acceptable approximation.

The simulation results for the 4WRSE-10 proportional valve are not entirely satisfactory. It can be assumed that this oscillation is due to the lack of amplitude incensing. The curves indicate that there is no excitation frequency at which the output amplitude is amplified, which points to the need for a different approach that could lead to better results.

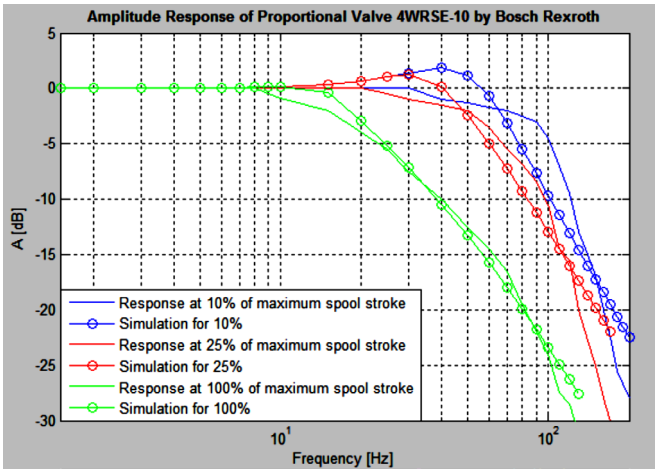

Figure 19. Amplitude Response for 4WRSE-10

3.3. Static model

In addition to the dynamic behaviour, it is also necessary to determine the static behaviour of the proportional valve. Static behaviour describes the relationship between flow and pressure loss. The valve can be seen as a built-in part. Embedded parts are components that are mounted in the pipework system of a hydraulic circuit. They can be fittings, nozzles, ports, valves, or filters. Thus, each incorporated part has its own friction factor ζ characteristics. The friction factor describes the relationship between the pressure loss Δp_{Loss} and the flow

rate Q. However, there is no universal approach to pre-calculating the pressure loss as a function of flow rate for each incorporated part. Apart from straight pipes, the exceptions are nozzles and orifices. The other components are geometrically more complex, which makes a theoretical approach difficult.

The general equilibrium approach, provided according to Bernoulli's law, from the inlet to the outlet of a given component, taking pressure loss into account, will be expressed as follows:

$$p_1 = p_2 + \frac{1}{2}\rho\, v^2\, \zeta = p_2 + \frac{1}{2}\rho \frac{Q^2}{A_p^2}\, \zeta \qquad (30)$$

On the other hand, if we consider that the dynamic pressure at the inlet and outlet, as well as the static pressure height terms, can be set to zero, the flow rate can be determined by (30). Where factor A_p represents the oil passage area of the valve, which depends on the position of the coil. The size of the area directly affects the value of the pressure loss factor ζ. While the pressure loss depends on the Reynolds number, which is a function of the flow rate.

Considering that the behaviour of the valve is divided into two sections that reflect the displacement of the coil and the different behaviours. At the transition point, the position of the coil between $-1 \leqslant \bar{x_s} \leqslant x_t$, the valve blocks the passage of oil, allowing only a small amount of leaked oil to pass through. However, if the coil is about to reach the transition point, its behaviour becomes non-linear due to manufacturing tolerances that cannot be avoided. On the other hand, if the coil displacement exceeds the transition point, the behaviour is strictly linear, the main characteristic of a proportional valve. From these considerations, it turns out that it is necessary to find two functional equations for the section before and after the x_t transition. The section before the transition can be approximated by:

$$A(-1 \leq \bar{x}_s \leq x_t) = ae^{b\bar{x}_s} \qquad (31)$$

here a and b are used to adjust the function to the valve's characteristics. In turn, the after section can be approximated using a linear function with a small deviation given by:

$$A(x_t < \bar{x}_s \leq 1) = c \cdot \bar{x}_s + d \qquad (32)$$

All these restrictions must be translated into a model that represents the behaviour of the proportional valve, considering all the flows and pressures, as shown in Figure 20(a). Figure 20(b) shows the typical graph of the Pseudo-Section Function of a paired symmetrical valve.

According to Figure 20(a) it is assumed that $Port_1$ is connected to the actuator's advance chamber while $Port_2$ is connected to the rod chamber with different inlet and outlet pressures and flow rates. The flow rate of oil, Q_1, entering the advance chamber under high pressure promotes the advance of the cylinder and, consequently, a return flow, Q_2, to the tank at a lower pressure. Thus, the inlet flow, Q_s, generated by the pump is divided into two leakage flows q_{s1} and q_{s2} that flow into the high and low-pressure chambers respectively. Where $Q_1 = q_s - q_{1t}$, $Q_2 = q_{2t} - q_{s2}$ and $Q_t = q_{1t} + q_{2t}$.

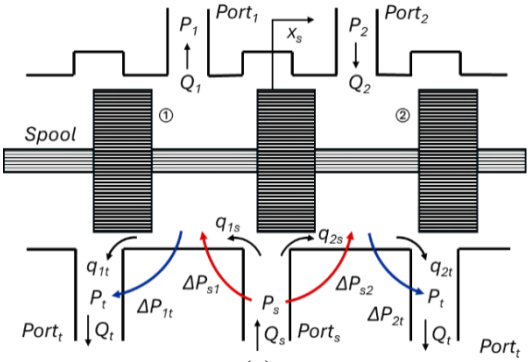

(a)

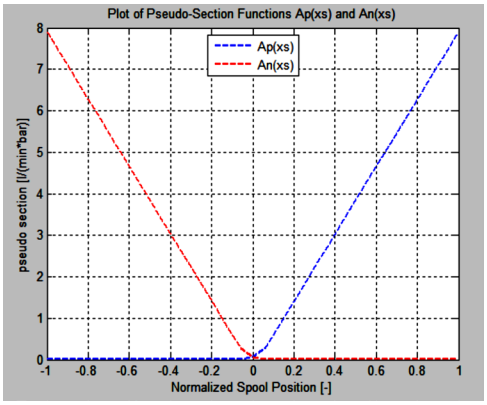

(b)

Figure 20. Valve 4WRSE-10: (a) Static Spool Position Model; (b) Pseudo-Section Function

Therefore, the pressure gain, $\bar{K}_{p0}$ (relative pressure gain at the middle spool position), can be understood as the derivative of the relative loading pressure with respect to the coil position which, in turn, is the ratio of the pressure difference between $Port_1$ and $Port_2$, while the flow gain, $\bar{K}_{q0}$ (relative flow gain in the middle spool position), will be determined by the derivative of the load flow under zero load pressure in the middle position.

Therefore, the pressure gain, $\bar{K}_{p0}$ (relative pressure gain at the middle spool position), can be understood as the derivative of the relative loading pressure with respect to the coil position which, in turn, is the ratio of the pressure difference between $Port_1$ and $Port_2$, while the flow gain, $\bar{K}_{q0}$ (relative flow gain in the middle spool position), will be determined by the derivative of the load flow under zero load pressure in the middle position.

4. Results and discussion

Different simulation approaches were used to study the static and dynamic behaviour of a proportional valve. The dynamic behaviour was implemented with a non-linear model in Simulink from a second-order linear system, adding saturation blocks for velocity and acceleration. On the other hand, as normalized inputs were used, it was not necessary to implement static gain factors. However, several other functions had to be implemented to optimize the non-linear model. These functions were used to filter the model's non-linear output signal for its excitation frequency and determine the intersection and zero matrices needed to calculate the amplitude and phase deviation. This optimization approach was then applied to the Bosch 4WRSE-10 valve, the only one in our laboratory, which showed promising results by stabilizing the objective function at around 1050 for the different sets of initial values. However, to develop the static model, it was necessary to determine the characteristics of the pressure and flow gain in the intermediate position, as well as the leakage flows. Based on the characteristics of the valve leaf, various non-linear equations were solved to obtain the pseudo-section functions that describe the relationship between the position of the coil and the flow rate.

Based on the above, modelling a proportional hydraulic system requires precise knowledge of all the parameters involved, from the inputs and outputs to the storage elements. All this knowledge is fundamental both for defining the equilibrium equations and the static relationships that make it possible to create the block model, which in this study was created in Matlab. Therefore, in addition to modelling all the hydraulic components, it is necessary to understand the functionality of the LVDT, which translates the input voltage into a linear displacement of the spool, the main requirement for the valve's control capability, that could be controlled/monotonized by a Programmable Logic Controller (PLC) [40]. On the other hand, it is also necessary to consider that these movements of the valve body cause the excitation frequency to overlap with the natural frequency of the system, disappearing over time due to the transient effect. It was also pointed out that all these considerations are necessary in order to evaluate the waveform in the simulation in time and frequency domain. The link between time and frequency was highlighted through the use of using the Fourier transform. Having said that, it is necessary to understand how the system works and where there are cut-off points between the various parts. This helps to divide the main system into subsystems, which simplifies the process of building models and simulating them, in a closed circuit, due to their lower complexity. It then becomes clear that small oscillations in the system influence the behaviour of the viscosity of the oil, usually HLP 46, which is directly related to the temperature or pressure that directly influences the mass.

The hydraulic cylinder model was modelled to create a general model that could respond to the inlet and outlet flow models and represent the dynamic balance of forces. This balance includes the friction force considering the static and dynamic friction coefficients [41] and a decay constant that verifies the extensibility of the piston at a constant speed.

As already mentioned, the proportional valve was modelled by subdividing it into a static valve model and a dynamic valve model. This subdivision is due to its non-linearity, which led to the non-linear dynamic behaviour being modelled using a second-order model with velocity and acceleration saturation. Using dynamic variables in Matlab's *fminsearch* optimization function, it was possible to find the best model parameters that minimized the error between the measured data points obtained from the frequency response curves and the Simulink model. The use of various excitation frequencies in the non-linear model caused harmonics which had to be filtered out. In addition, intersection functions, zero matrices, amplitude calculation and phase deviation were tested to create simulated frequency response curves in order to compare simulation with reality. The correct functionality of these functions was demonstrated for the optimization of a second-order linear model. However, the optimization for the Bosch 4WRSE-10 valve showed slight deviations for the amplitude response of 10% and 25% of the maximum coil travel.

For the static model, the pressure, flow, and leakage gain, as well as the supply and nominal pressure, had to be determined from the valve data sheet. With this approach, it was possible to solve the non-linear equations that describe the behaviour of the positive and negative pseudo-section functions. These can be understood as conductance values that provide information about the flow through the valve at a given standardized spool position. The methodologies and models developed were tested with data from the manufacturer and the results were good, which corroborated the adopted approach. It is also possible to consider that the approach presented here can be extrapolated to any other proportional valve, considering all the relevant operating data, i.e. precise knowledge of all the parameters involved, from the inputs and outputs to the storage elements.

5. Conclusion

This study presents the presents a mathematical model for the piston position of an Electro-Hydraulic Proportional System, utilizing the Matlab/Simulink framework. The model describes the behaviour of the entire hydraulic valve assembly (valve, spool position transducer and electronic controller cart). Several decoupled models are used which translate the static behaviour of the valve as a function of the flow through it and the positioning of the coil and pressure losses. The flow was modelled as laminar and modelled by pseudo-section functions. The dynamic sub model describes the displacement of the coil when an input signal is applied.

The adaptability of the model was tested in both static and dynamic terms using a second-order model with

saturated velocity and acceleration with dynamically and perfectly adjustable variables. The valve parameters of the static model can be calculated directly from the manufacturer's data or from experimental measurements, since they were not considered as constants, but as variables. The dynamic behaviour was determined by optimization techniques based on the manufacturer's Bode diagrams. The suitability of the model was demonstrated, leading to good results, in line with those obtained by [37]. The suitability for the proportional Bosch 4WRSE-10 valve proved to be very promising in terms of the amplitude response of the coil curve.

Proportional valves are economical and robust components with high potential for use in industrial automation applications and in environments where precision is critical, and cost restrictions apply. On the other hand, their applicability in the fields of automation, mechanical engineering and the design of hydraulic circuits to replace servo-valves stands out. We can also consider that the use of proportional valves meets industrial sustainability and energetic efficiency trends of the hydraulic system (Industri 5.0), both in terms of the data predictive maintenance, digital twins (Industri 4.0) and environmental restrictions, contributing to an alignment between theoretical modelling and the practical industrial application of advanced hydraulic control.

To continue this work in the future, several tasks need to be carried out. The friction force model for the hydraulic cylinder is based on assumptions that need to be corrected. With this data, the friction force model needs to be better adapted to the actual behaviour. This can be achieved by changing certain parameters, such as the decay constant T_V. It should be mentioned that the extension and shrinkage characteristics are probably not the same.

The Simulink model for obtaining the dynamic behaviour of the proportional directional valve needs to be better adapted to the curves in the data sheet. Therefore, provides approaches that may be useful for additional considerations. It is recommended to determine the phase deviation using a time delay constant. This constant should be optimized for the manufacturer's curves. Finally, the different models should be linked together. It will be also important in the future to validate the model the built model by comparison with a real hydraulic circuit in different conditions.

Acknowledgements.

This work was partially financially supported by FCT—Fundacão para a Ciência e Tecnologia (Portugal), who partially financially supported this work through the RD Units Project Scope: UIDP/04077/2020 and UIDB/04077/2020. The authors are grateful, too, to the partial financial support provided by Base Funding—UIDB/50022/2020 (LAETA) of INEGI—Institute of Science and Innovation in Mechanical and Industrial Engineering, Portugal.

References

[1] Sârbu FA, Arnăuţ F, Deaconescu A, Deaconescu T. Theoretical and Experimental Research Concerning the Friction Forces Developed in Hydraulic Cylinder Coaxial Sealing Systems Made from Polymers. Polymers 2024; 16(1):157. https://doi.org/10.3390/polym16010157.

[2] Xuan Bo Tran, Nur Hafizah, Hideki Yanada. Modeling of dynamic friction behaviors of hydraulic cylinders. Mechatronics 2012; *212*(1):65-75. https://doi.org/10.1016/j.mechatronics.2011.11.009.

[3] Jaiswal, S., Sopanen, J. & Mikkola, A. Efficiency comparison of various friction models of a hydraulic cylinder in the framework of multibody system dynamics. Nonlinear Dyn 2021; 104:3497–3515. https://doi.org/10.1007/s11071-021-06526-9.

[4] Xuyao Mao, Wei Duan, Chao Xiang, Chao Wu1 and Ze Wang. Design and Simulation of a Position and Average Velocity Closed-loop Control Method of a Hydraulic Servo System. Journal of Physics: Conference Series 2022; 2364:012061. https://doi.org/10.1088/1742-6596/2364/1/012061.

[5] Wonohadidjojo, D.M., Kothapalli, G. & Hassan, M.Y. Position Control of Electro-hydraulic Actuator System Using Fuzzy Logic Controller Optimized by Particle Swarm Optimization. Int. J. Autom. Comput. 2013; 10:181–193. https://doi.org/10.1007/s11633-013-0711-3.

[6] Santhosh K. R, M. Kumar, Sireesha Koneru. Simulation of Hydraulic Circuits by using Matlab-Simulink Software. Int. Jour. of Mech. and Prod. Eng. Res. and Dev. (IJMPERD) 2019; 9(3):1643-1654. doi:10.24247/ijmperdjun2019173.

[7] Tony Thomas, A., Thangarasu, S.K., Sowmithra, T. Modeling and Simulation of an Electro-Hydraulic System Using Fuzzy Logic Approach. In: Prabu, T., Viswanathan, P., Agrawal, A., Banerjee, J. (eds) Fluid Mechanics and Fluid Power. Lecture Notes in Mechanical Engineering. Springer, Singapore 2021; pp. 807-822. https://doi.org/10.1007/978-981-16-0698-4_89.

[8] Sahu GN, Singh S, Singh A, Law M. Static and Dynamic Characterization and Control of a High-Performance Electro-Hydraulic Actuator. Actuators 2020; 9(2):46. https://doi.org/10.3390/act9020046.

[9] Zhang Z, Du H, Chen S, Huang H. Frequency domain modeling, analysis and verification of electro-hydraulic servo steering system for heavy vehicles. Proceedings of the Institution of Mechanical Engineers, Part D: Journal of Automobile Engineering **2020**; 234(12):2836-2850. doi:10.1177/0954407020918696.

[10] Erzan Topçu E. PC-based control and simulation of an electro-hydraulic system. Comput Appl Eng Educ. 2017; *25*:706–718. https://doi.org/10.1002/cae.21831.

[11] Xianju Yuan, Sixiu Shi, Chuyan Wang, Lifeng Wei, Chen Luo, Junjie Chen. Dynamic modeling method for an electro-hydraulic proportional valve coupled mechanical–electrical-electromagnetic-fluid subsystems. Journal of Magnetism and Magnetic Materials 2023; 587:171312. https://doi.org/10.1016/j.jmmm.2023.171312.

[12] Li X, Zhang L, Yang S, Liu N. Analysis and experiment of HMT stationary shift control considering the effect of oil bulk modulus. Advances in Mechanical

Engineering 2020; 12(11). doi:10.1177/1687814020968324.
[13] Noah D. Manring, Roger C. Fales. Hydraulic Control Systems, 2nd Edition. John Wiley & Sons: Hoboken, NJ, USA, 2019.
[14] Boulet, B., Daneshmend, L., Hayward, V., Nemri, C. System Identification and Modelling of a High Performance Hydraulic Actuator. Springer: Berlin/Heidelberg Germany. 1993.
[15] Bing Xu, Qi Su, Junhui Zhang, Zhenyu Lu. Analysis and compensation for the cascade dead-zones in the proportional control valve. ISA Transactions 2017; 66:393-403. https://doi.org/10.1016/j.isatra.2016.10.012.
[16] Habibi, S.; Goldenberg, A. A mechatronics approach for the design of a new high performance electrohydraulic actuator. SAE Trans. 1999; 108:353–360. http://www.jstor.org/stable/44723058.
[17] Jianyong, Y.A.; Zongxia, J.I.; Bin, Y.A. Robust control for static loading of electro-hydraulic load simulator with friction compensation. Chin. J. Aeronaut 2012; 25:954–962. https://doi.org/10.1016/S1000-9361(11)60467-6.
[18] Huang J, Song Z, Wu J, Guo H, Qiu C, Tan Q. Parameter Adaptive Sliding Mode Force Control for Aerospace Electro-Hydraulic Load Simulator. Aerospace 2023; 10(2):160. https://doi.org/10.3390/aerospace10020160.
[19] Yuan, H.; Na, H.; Kim, Y. System identification and robust position control for electro-hydraulic servo system using hybrid model predictive control. J. Vib. Control 2018; 24:4145-4159. https://doi.org/10.1177/1077546317721417.
[20] Wang, H., Wang, X., Huang, J. *et al.* Flow Control for a Two-Stage Proportional Valve with Hydraulic Position Feedback. Chin. J. Mech. Eng. 2020; 33:93. https://doi.org/10.1186/s10033-020-00517-4.
[21] Siddique MAA, Kim W-S, Kim Y-S, Kim T-J, Choi C-H, Lee H-J, Chung S-O, Kim Y-J. Effects of Temperatures and Viscosity of the Hydraulic Oils on the Proportional Valve for a Rice Transplanter Based on PID Control Algorithm. Agriculture 2020; 10(3):73. https://doi.org/10.3390/agriculture10030073.
[22] Li N, Ji H, Wei L, Dong W, Zhan P, Liu X. Generation mechanism of high-frequency oscillation in proportional valve with a high-speed on/off valves bridge as the pilot stage. Proceedings of the Institution of Mechanical Engineers, Part C: Journal of Mechanical Engineering Science 2024; 238(9):4033-4043. https://doi.org/10.1177/09544062231200694.
[23] William de Paula Ferreira, Fabiano Armellini, Luis Antonio De Santa-Eulalia. Simulation in industry 4.0: A state-of-the-art review. Computers & Industrial Engineering 2020; 149:106868.https://doi.org/10.1016/j.cie.2020.106868.
[24] Wagg, D. J., Worden, K., Barthorpe, R. J., and Gardner, P. Digital Twins: State-of-the-Art and Future Directions for Modeling and Simulation in Engineering Dynamics Applications. ASME J. Risk Uncertainty Part B 2020; 6(3):030901. https://doi.org/10.1115/1.4046739.
[25] Santos, Adriano A., Pereira, F. and Felgueiras, C. Optimization and improving of the production capacity of a flexible tyre painting cell. Int J Adv Manuf Technol 2024; 13(9):3957-3969. https://doi.org/10.1007/s00170-024-13208-4.
[26] Lunze, J. Zielstellung und theoretische Grundlagen der Regelungstechnik. In: Regelungstechnik 1. Springer Vieweg, Berlin, Heidelberg, 2020, pp. 1-19. https://doi.org/10.1007/978-3-662-60746-6_1.
[27] Norbert Gebhardt, Jürgen Weber. Hydraulik – Fluid-Mechatronik; Grundlagen, Komponenten, Systeme, Messtechnik und virtuelles Engineering. Springer Vieweg Berlin, Heidelberg 2020. https://doi.org/10.1007/978-3-662-60664-3.
[28] H. Watter. Hydraulik und Pneumatik, Grundlagen und Übungen - Anwendungen und Simulation, 6 ed. Wiesbaden: Springer Vieweg, 2022. https://doi.org/10.1007/978-3-658-35866-2.
[29] Bora Eryilmaz, Bruce H. Wilson. Unified modeling and analysis of a proportional valve. Journal of the Franklin Institute 2006; 343(1):48-68. https://doi.org/10.1016/j.jfranklin.2005.07.001.
[30] D. Will, H. Ströhl und N. Gebhardt, Hydraulik - Grundlagen, Komponenten, Schaltungen, 7 ed. Berlin: Springer, 2020. https://doi.org/10.1007/978-3-662-60664-3.
[31] Hao Xu, Bin Meng, Chenhang Zhu, Yaozhen Heng, and Jian Ruan. Multi-objective optimization design of two-dimensional proportional valve with magnetic coupling. Advances in Mechanical Engineering 2022; 14(11):1-18. https://doi.org/10.1177/16878132221134986.
[32] Bosch Rexroth. 4/3 directional high-response control valves, RE 29067/11.05. https://www.boschrexroth.com/media/ccb8ea97-7f84-40b6-a76d-d2a5c4ae3389 last accessed 03 March 2025.
[33] National Instruments. Position & Displacement Measurement with LVDTs. https://www.ni.com/en/shop/data-acquisition/measuring-position-and-displacement-with-lvdts.html last accessed 04 March 2025.
[34] N. Hanson. Hydraulic Proportional and Closed Loop System Design, Bosch Rexroth. https://www.cmafh.com/enewsletter/pdfs/dch_hydraulicproportional.pdf last accessed 4 March 2025.
[35] P. Beater. Entwurf hydraulischer Maschinen - Modellbildung, Stabilitätsanalyse und Simulation hydrostatischer Antriebe und Steuerungen. Springer Berlin, Heidelberg, 1999. https://doi.org/10.1007/978-3-642-58395-7.
[36] Aboelela, M. A. S., Essa, M. E. S. M., & Hassan, M. A. M. Modeling and identification of hydraulic servo systems. International Journal of Modelling and Simulation 2018; 38(3):139–149. https://doi.org/10.1080/02286203.2017.1405713.
[37] Ferreira, J. A., De Almeida, F. G., & Quintas, M. R. Semi-empirical model for a hydraulic servo-solenoid valve. Proceedings of the Institution of Mechanical Engineers, Part I: Journal of Systems and Control Engineering 2002; 216(3): 237-248. https://doi.org/10.1177/095965180221600303.
[38] MathWorks – Help Center Homepage, https://www.mathworks.com/help/matlab/ref/fminsearch.html, last accessed 4 March 2025.
[39] J. A. F. Ferreira: Modelação de sistemas hidráulicos para simulação com hardware-in-the-loop. Ph.D.

Thesis. Universidade de Aveiro, Portugal 2002. http://hdl.handle.net/10773/10859.

[40] Graça Sobral: Desenvolvimento de uma interface gráfica para controlo de uma válvula direcional proporcional. Master Thesis. Instituto Politécnico do Porto, Portugal 2018. https://recipp.ipp.pt/entities/publication/3229d785-91a5-4559-8a08-cc0817a569af.

[41] Formelsammlung und Berechnungsprogramme Maschinen- und Anlagenbau, Reibwerte von verschiedenen Materialien Homepage, https://www.schweizer-fn.de/stoff/reibwerte/reibwerte.php last accessed 4 March 2025.